

5. H. Liu, J. Kohler, G. R. Fink, *Science* **266**, 1723 (1994).
6. S. J. Kron and N. A. Gow, *Curr. Opin. Cell. Biol.* **7**, 845 (1995); J. R. Köhler and G. R. Fink, *Proc. Natl. Acad. Sci. U.S.A.* **93**, 13223 (1996); E. Leberer *et al.*, *ibid.*, p. 132217.
7. F. E. Williams and R. J. Trumbly, *Mol. Cell. Biol.* **10**, 6500 (1990).
8. C. A. Keleher, M. J. Redd, J. Schultz, M. Carlson, A. D. Johnson, *Cell* **68**, 709 (1992).
9. J. F. Lemontt, D. R. Fugit, V. L. Mackay, *Genetics* **94**, 899 (1980).
10. D. Tzamaras and K. Struhl, *Nature* **369**, 758 (1994); K. Komachi, M. J. Redd, A. D. Johnson, *Genes Dev.* **8**, 2857 (1994); M. Wahi and A. D. Johnson, *Genetics* **140**, 79 (1995); D. G. Edmondson, M. M. Smith, S. Y. Roth, *Genes Dev.* **10**, 1247 (1996).
11. PCR primers used to amplify a fragment of *C. albicans TUP1* were: 5'GGGGTACCCYTTCCADAT-NCKNGCYTTRCARTCNCC, coding in reverse for COOH-terminal GDCKARIWK, [A. Cornish-Bowden, *Nucleic Acids Res.* **13**, 3021 (1985)]; and 5'GGCT-GCAGGGNCAYGARCARGAYATHTTAYTC, coding for NH₂-terminal GHEQDIYS. Cycling parameters were 1 min at 95°C, 1 min at 55°C, 1 min ramp to 73°C, and 3 min at 73°C (Perkin-Elmer Cetus 480 cycler). The resulting 659-bp PCR fragment was cloned via the Pst I and Kpn I sites on the ends into Bluescript-derived pVZ1 to produce p348. A library of *C. albicans* genomic DNA was provided by N. Agabian and colleagues (UCSF), and was screened with labeled insert from p348. A 7-kbp *TUP1*-containing Kpn I-Xba I fragment from λ 363 was cloned into pVZ1 to form p371. Both strands of the *TUP1* open reading frame were sequenced. The *C. albicans TUP1* DNA and protein sequences have been deposited in GenBank (AF005741).
12. M. A. Wall *et al.*, *Cell* **83**, 1047 (1995).
13. The *C. albicans TUP1* open reading frame was amplified with Pfu polymerase (Stratigene) and the primers: 5'CGGGATCCCCACCCAGCAATGTCCATGTAT; 5'GCGGGTACCGCGATGTTGACGGGTGCTGT. The product was cloned into the *CEN/ARS/URA3/Gal1-10* expression vector pRD53 (provided by R. Deshaies, California Institute of Technology) to form the *S. cerevisiae* expression plasmid pMH1. *C. albicans TUP1* contains no CUG codons, which encode serine in *C. albicans*, but encode leucine in *S. cerevisiae* and elsewhere [T. Ohama, *et al.*, *Nucleic Acids Res.* **21**, 4039 (1993)]. The same PCR product was cloned into pDBV52 (provided by C. Kumamoto and D. Brown, Tufts) to form the maltose-regulated expression plasmid p455, which was transformed into BCa2-9. pAJ181 has been described (8). To assess *TUP1* function, β -galactosidase activity was assayed from *tup1 S. cerevisiae* (KKY110) carrying the plasmids described above. KKY110 (*Mata*, *tup1*, *mfa2::lacZ*, *leu2*, *ura3*, *trp1*, *his4*; provided by K. Komachi, UCSF) had a β -galactosidase reporter gene under $\alpha 2/MCM1/TUP1$ control integrated at the *MFA2* gene. On glucose, the vector (pRD53) conferred 82 \pm 16 units, (no repression); pAJ181 (*S. cerevisiae TUP1*) conferred 3.8 \pm 0.9 units; and pMH1 (Gal-driven *C. albicans TUP1*) conferred 32 \pm 5 units. On galactose, the vector conferred 83 \pm 27 units (no repression); pAJ181, 0.7 \pm 0.5 units; and pMH1, 0.5 \pm 0.4 units (full repression).
14. W. A. Fonzi and M. Y. Inwin, *Genetics* **134**, 717 (1993). The *C. albicans URA3* gene, flanked by tandemly repeated DNA sequences, was inserted in place of *TUP1* within the genomic clone (Fig. 2A) to form p383C, which was treated with Sph I to remove the vector and transformed into a *ura3 C. albicans* cell (CAI4). The *URA3* transformants were screened by DNA blotting for disruption of one *TUP1* gene by homologous recombination. After being selected on 5-FOA for *ura3* "pop-out" revertants, a second cycle of transformation was performed. DNA blotting revealed the successive disruption of both copies of the *TUP1* gene (Fig. 2B, compare lanes 2, 3, and 6). Transformations of *S. cerevisiae* were done by a modified lithium acetate technique [R. D. Gietz, R. H. Schiestl, A. R. Willems, R. A. Woods, *Yeast* **11**, 355 (1995); J. Hill, K. A. Donald, D. E. Griffiths, G. Donald, *Nucleic Acids Res.* **19**, 5791 (1991)]. Transformation of *C. albicans* was identical, except that DMSO was omitted, incubation times at 30°C and 42°C were extended to 3 hours and 1 hour, respectively, and uridine at 25 μ g/ml was added to the plating solution. All *C. albicans* strains shared the SC5314 background. The *C. albicans* allele *tup1:hisG* described is referred to as *tup1 Δ -1*.
15. Cells were fixed for microscopy with 70% ethanol, rinsed twice in water, and incubated in 4',6-diamidino-2-phenylindole hydrochloride (DAPI) (250 ng/ml) or calcofluor white M2R (a boshork) (500 μ g/ml) for 10 min at room temperature. DAPI-stained cells were rinsed once before mounting in 50% glycerol, and calcofluor-stained cells were rinsed four times. Fluorescence and differential interference contrast micrographs were taken on a Nikon Optiphot microscope with 40 \times and 100 \times objectives with DAPI-specific illumination and filters. Micrographs of cells on plates were taken on an Olympus BX40 microscope, with 10 \times and 40 \times objectives with phase. We used the Dalmat plate technique to investigate filamentous growth from colonies of *C. albicans* [M. R. McGinnis, *Laboratory Handbook of Medical Mycology* (Academic Press, New York, 1980)].
16. Standard yeast media such as yeast extract with peptone and dextrose (YEPD) were made as described [F. Sherman, in *Guide to Yeast Genetics and Molecular Biology*, C. Guthrie and G. R. Fink, Eds. (Academic Press, San Diego, 1991), vol. 194, p. 3]. Uridine (25 μ g/ml) was added to 5-fluoroorotic acid plates used to counter-select against *URA3* in *C. albicans*. SLAHD (19), Spider (5), and Lee's (17) media were made as described. Saboraud dextrose agar and cornmeal agar (Difco) plates were made to manufacturer's directions, with added 0.33% Tween 80 (16).
17. K. L. Lee, H. R. Buckley, C. C. Campbell, *Sabouraudia* **13**, 148 (1975).
18. L. A. Merson-Davies and F. C. Odds, *J. Gen. Microbiol.* **135**, 3143 (1989).
19. C. J. Gimeno, P. O. Ljungdahl, C. A. Styles, G. R. Fink, *Cell* **68**, 1077 (1992).
20. R. L. Roberts and G. R. Fink, *Genes Dev.* **8**, 2974 (1994); R. M. Wright, T. Repine, J. E. Repine, *Curr. Genet.* **23**, 388 (1993).
21. Obtained from G. Fink and colleagues.
22. *S. cerevisiae* disruptions were carried out with marked fragments from the plasmids pFW40 [URA3 (7)] and pCK36 [LEU2 (8)]. All *S. cerevisiae* strains but KKY110 shared the Σ 1278b pseudohyphal-competent background (19). KKY110 (K. Komachi; UCSF) derives from EG123. Pseudohyphal-competent strains L5684 and L5487 (provided by G. Fink and colleagues; Whitehead Institute) were mated by micromanipulation to create diploid BB8, which was sequentially transformed to disrupt both copies of *TUP1*. Alterations at the locus were assayed by whole-cell PCR with appropriate oligonucleotides.
23. Preliminary results indicate that mutant *tup1 C. albicans* (BCa2-10;*tup1/tup1*, *URA3/ura3*) are far less infectious in mice than are the parental wild-type (SC5314) cells. This lack of infectivity could be due to constitutive filamentous growth, lack of germ tube formation, or other defects of the mutant strain (P. L. Fidel, Jr., B. R. Braun, and A. D. Johnson, unpublished data).
24. We thank N. Agabian, W. Fonzi, T. Brake, G. Fink, C. Kumamoto, D. Brown, and members of the Johnson laboratory for materials; J. Edman and P. O'Farrell for microscope facilities; T. White, M. McEachern, T. Sherman, and members of the Johnson laboratory for assistance and discussions; and M. Hooper for help in construction of the *S. cerevisiae* expression clone. Supported by an American Cancer Society postdoctoral fellowship (B.R.B.), and by NIH grant GM37049 (A.D.J.).

16 September 1996; accepted 26 February 1997

Modulation of Hepatic Gene Expression by Hepatocyte Nuclear Factor 1

Eleni Ktistaki and Iannis Talianidis*

Hepatocyte nuclear factors 1 and 4 (HNF-1 and HNF-4) are liver-enriched transcription factors that function in the regulation of several liver-specific genes. HNF-1 activates genes containing promoters with HNF-1 binding sites. However, this factor negatively regulates its own expression and that of other HNF-4-dependent genes that lack HNF-1 binding sites in their promoter region. This repression is exerted by a direct interaction of HNF-1 with AF2, the main activation domain of HNF-4. The dual functions of gene activation and repression suggest that HNF-1 is a global regulator of the transcriptional network involved in the maintenance of hepatocyte-specific phenotype.

Liver-specific gene expression is governed by the combinatorial action of a small set of liver-enriched transcription factors, including HNF-1, C/EBP, HNF-3, and HNF-4 (1). The expression patterns of HNF-1 and HNF-4 closely correlate with the differentiation state of hepatic cells. HNF-4 is an activator of the HNF-1 gene, defining a transcriptional hierarchy involved in both the determination and maintenance of hepatic phenotype (2). In transient transfection experiments, HNF-1 negatively regu-

lates its own and other HNF-4-dependent promoters that are not directly recognized by HNF-1 (3). These findings suggested the functioning of an indirect negative autoregulatory mechanism that is triggered by increased intracellular concentrations of HNF-1. HNF-1 did not affect several other promoters, and fusion proteins containing different NH₂- and COOH-terminal parts of the HNF-1 molecule failed to inhibit HNF-4-mediated transcription (3, 4). These findings argue against a squelching effect.

To investigate the potential role of HNF-1 on the transcription of its own gene in the *in vivo* chromosomal context, we generated stable HepG2 cell lines (H1A

Institute of Molecular Biology and Biotechnology, Foundation for Research and Technology-Hellas, Post Office Box 1527, 711 10 Heraklion, Crete, Greece.

*To whom correspondence should be addressed.

and H1B) expressing different amounts of HNF-1 protein. The expression of endogenous HNF-1 and various target genes was analyzed by Northern (RNA) blot analysis. A glyceraldehyde phosphate dehydrogenase (GAPDH) probe that produced constant amounts of mRNA was used as a control. Hybridization with a probe encompassing the coding region of the rat HNF-1 cDNA (rHNF-1CR) produced signals of 3.6 and 3.0 kb that corresponded to endogenous and transgene-derived HNF-1, respectively (Fig. 1). The amount of endogenous HNF-1 transcript was reduced in both H1A and H1B cell lines. This decrease was also observed by hybridization with the use of a 3' untranslated (3' UTR) fragment of the human HNF-1 as a probe that detected only endogenous HNF-1 mRNA (Fig. 1). Expression of apolipoprotein C-III (apoC-III) is dependent on HNF-4 (5). The amount of apoC-III mRNA was decreased in the HNF-1-overproducing cell lines. However,

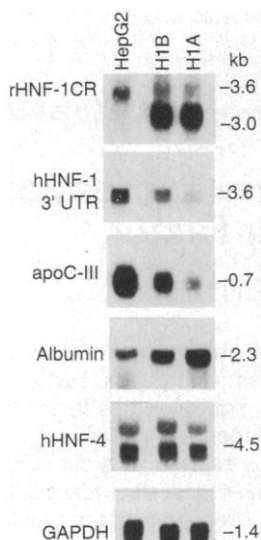


Fig. 1. Ectopic expression of HNF-1 represses endogenous HNF-1 and apoC-III transcription. HepG2 cells were transfected with pCB-HNF-1 expression vector (3), and stably expressing cell lines were selected and expanded in a medium containing G418 (150 μ g/ml; Geneticin, BRL). Polyadenylate RNAs from cell lines expressing different amounts of HNF-1 (H1A and H1B) were prepared and compared with wild-type HepG2 mRNA by Northern blot hybridization using the following probes: rHNF-1CR (containing the entire coding region of rat HNF-1 cDNA), hHNF-1 3' UTR (containing nucleotides 2305 to 2783 of the 3' untranslated region of human HNF-1 cDNA), and cDNAs coding for human apoC-III, mouse albumin, human HNF-4 (hHNF-4), and GAPDH as control. Hybridization and washing conditions were as described in (13). Positions of radioactive signals are shown at the right. With HNF-4 a second signal above the 4.5-kb band can also be seen, which corresponds to cross-hybridization with contaminating 28S ribosomal RNA.

the hybridization signal for mRNA transcribed from the HNF-1-dependent albumin gene (6) was increased. The amount of HNF-4 transcript remained constant, which implied a lack of positive reciprocal activation of HNF-1 and HNF-4 in the chromosomal context. Consistent with this notion is the observation that some HNF-4 promoter constructs that contain the putative HNF-1 binding site do not drive liver-specific expression in transgenic mice (7). Moreover, wild-type and null mutant mice that are devoid of HNF-1 express HNF-4 in similar amounts (8).

In the HNF-1-overproducing cell lines, the activities of the albumin, apoC-III, and HNF-1 promoters were affected in the same way as the amount of their steady-state mRNA, indicating that the observed changes were the result of altered transcription rates (Fig. 2). In addition, the activity of the chimeric promoter construct 4xA TK-CAT, which contains four copies of the HNF-4 binding site of the HNF-1 promoter, was also reduced. On the other hand, the activity of the control promoter (RSV-CAT) was not changed (Fig. 2). This suggests that HNF-1 exerts its negative effect by counteracting HNF-4 activation on the corresponding regulatory regions.

Fig. 2. Negative regulation of HNF-4-dependent promoters by HNF-1. Wild-type (WT) and HNF-1-overexpressing HepG2 cell lines (B and A) were transfected by the calcium phosphate precipitation method (13) with 2 μ g of the indicated reporters containing the mouse albumin (Alb-CAT) (3), human apolipoprotein C-III (ApoC-III-CAT) (5, 13), rat HNF-1 (HNF-1-CAT) (3), or Rous sarcoma virus (RSV-CAT) (3) promoters, or a chimeric reporter construct containing four copies of the HNF-4 binding site of the HNF-1 promoter fused to the minimal promoter region (nucleotides -85 to +51) of the herpes simplex virus thymidine kinase gene (4xA TK-CAT) (3). The bars represent means \pm SE of normalized CAT (chloramphenicol acetyltransferase) activities from at least four independent experiments, and these values are expressed as relative activation (Alb-CAT) or as a percentage of the activity measured in wild-type cells.

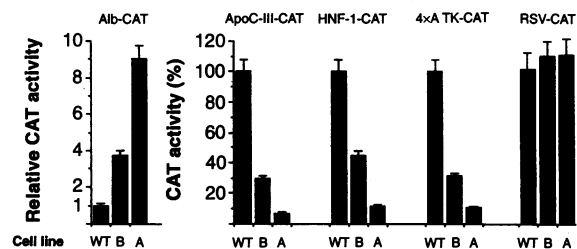
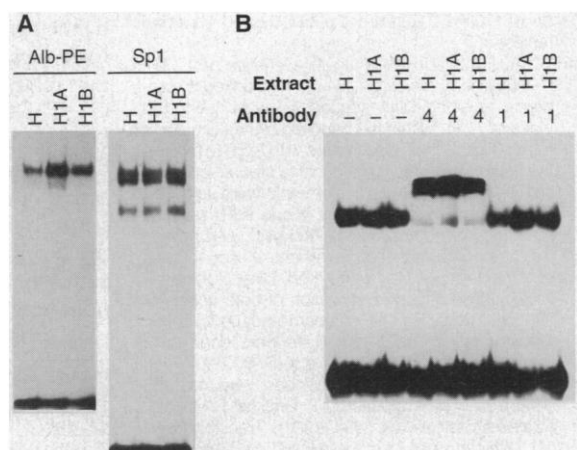


Fig. 3. Site A of the HNF-1 promoter binds HNF-4 but not HNF-1. Nuclear extracts from wild-type HepG2 (H) and the HNF-1-overexpressing (H1A and H1B) cell lines were prepared and analyzed in electrophoretic mobility shift assays using (A) Alb-PE and Sp1 or (B) site A oligonucleotide probes, as described (13). In some assays, 1 μ l of antibody to HNF-4 (4) or HNF-1 (1) at 1:6 dilution were also included. The identity of HNF-1 that bound to the Alb-PE probe was verified by supershifts with HNF-1 antibody (10).



To understand the molecular mechanism responsible for the above observations, we performed electrophoretic mobility shift assays to compare the amounts of active DNA binding protein in the stable cell lines. As a control, Sp1 binding activity was monitored and found to be similar in all extracts (Fig. 3A). Alb-PE (3, 6) and site A (3) were used as probes for HNF-1 and HNF-4, respectively. In the H1A and H1B cell lines, DNA binding to the Alb-PE probe was 11 and 4 times that of the wild type, respectively (Fig. 3A). This is much lower than the observed increase in total amounts of HNF-1 mRNA. The difference might result from additional translational control mechanisms or limiting intracellular concentrations of DCoH (dimerization cofactor for HNF-1), which is required for HNF-1 dimerization and stability (9). No difference in DNA binding activity on the HNF-4 probe was observed with the different HepG2 cell lines (Fig. 3B). An antibody raised against HNF-4 almost quantitatively supershifted the DNA-protein complex formed on the site A probe, whereas an HNF-1 antibody failed to supershift the complex (Fig. 3B). Moreover, no difference in HNF-4 binding affinity to site A was detected with the use of extracts from the

HepG2, H1A, and H1B cell lines or extracts from HNF-4⁻ and HNF-1-transfected COS-1 cells (10). Thus, neither HNF-1 nor another factor that may have been induced by HNF-1 interacts directly with site A, and HNF-1 does not affect the DNA binding activity of HNF-4.

Although mobility shift experiments did not reveal interactions between HNF-1 and HNF-4, weak protein-protein interactions may exist that are unable to survive electrophoretic conditions but could explain the down-regulation of HNF-4-dependent

genes by HNF-1. To test this idea, we mapped the HNF-4 protein domains necessary for HNF-1-mediated down-regulation. Fusion proteins containing the Gal4 DBD (the DNA binding domain of yeast Gal4 protein) and parts of HNF-4 bind to the Gal4 response element as dimers through the Gal4 DBD (11), and their expression is not affected by HNF-1 (10). The Gal4 HNF-4(E) construct that contains the complete ligand binding-dimerization domain (12) of HNF-4 was a potent activator of the Gal4-responsive reporter in both HepG2

and COS-1 cells (Fig. 4). This activation was strongly inhibited by increased intracellular amounts of HNF-1 derived from its ectopic expression in the stably transfected HepG2 cell lines (H1B and H1A) or from cotransfected expression vector (COS-1 cells). Similar results were obtained with cotransfected HNF-1(440), which lacks the COOH-terminal activation domains, whereas HNF-1(280), which contains the dimerization and DNA binding domains, failed to exhibit repressor activity (Fig. 4). Partial deletion of the main activation domain of HNF-4 [Gal4 HNF-4(E354)], which is located between amino acids 337 and 368, resulted in loss of activity. No significant change was observed in experiments with Gal4 VP16, which was used as an unrelated control (Fig. 4).

These results indicated that HNF-1 may repress gene expression through physical interaction with HNF-4. In vitro evidence for such protein-protein interaction was provided by pull-down assays with glutathione-S-transferase (GST)-HNF-4 fusion proteins and in vitro synthesized ³⁵S-labeled HNF-1. HNF-1 associated with TFIIB (Fig. 5A); this interaction may be important for HNF-1-facilitated formation of preinitiation complexes. Comparable amounts of bound HNF-1 protein were recovered by GST-HNF-4(130-368), containing the entire E domain, and by GST-HNF-4(AF2), containing the main activation region (amino acids 337 to 368) of HNF-4. In contrast, no interaction was observed with an HNF-4 derivative lacking the AF2 domain [GST-HNF-4(ΔAF2)] or with the GST-Gal4 fusion protein that was used as an unrelated control (Fig. 5A).

Interaction between HNF-4 and HNF-1 in intact cells was determined by nuclear cotranslocation assays with the use of a mutant form of HNF-4 [HNF-4(227-455)], which lacks specific nuclear localization signals but contains the domain required for in vitro interaction with HNF-1. This mutant was detected exclusively in the cytoplasm of transfected COS-1 cells (Fig. 5B). Coexpression of HNF-4(227-455) with either full-length HNF-1 (FL) or HNF-1(440), but not with HNF-1(280) or Gal4 protein, resulted in its translocation to the nucleus (Fig. 5B). Thus, HNF-1-HNF-4 interaction required the HNF-1 domain located between amino acids 280 and 440, but not the COOH-terminal activation domains of HNF-1.

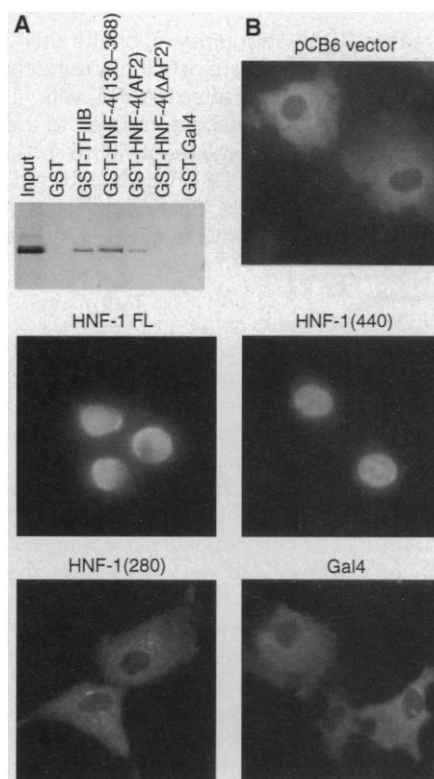
Taken together, our results indicate that the AF-2 domain of HNF-4 is sufficient and necessary for physical interaction with HNF-1 and for repression. This association may block the HNF-4 activation domain in a way that prevents either its interaction with coactivators that transduce AF2 activ-

Fig. 4. HNF-1 represses HNF-4 activity through interaction with the HNF-4 E domain in vivo. COS-1 and HepG2 lines (WT, H1B, H1A) were transfected with 2 μg of G4-CAT reporter containing four copies of the 17-nucleotide oligomer

Gal4 binding site, together with 0.5 μg of the indicated Gal4 expression plasmids. In COS-1 cells, 0.5 μg of pCB-HNF-1 (FL), pCB-HNF-1(280) (M280), or pCB-HNF-1(440) (M440) was also included where indicated. The numbers represent mean values of β-galactosidase-normalized CAT activities from at least six independent experiments with SEs of <8% and are expressed as activation relative to the activity obtained with the Gal4 DBD. Maximal activity in both HepG2 and COS-1 cells was obtained with a fusion construct containing the entire E domain [Gal4 HNF-4(E)]. No activity was observed when other combinations of HNF-4 domains (such as amino acids 337 to 368, 337 to 455, 368 to 455, and 227 to 455) were tested, suggesting that the HNF-4 AF2 domain is active only in the context of an intact E domain (14).

	Gal4 DBD	COS-1 cells						
		HepG2 cell lines			+HNF-1			
		WT	H1B	H1A	-HNF-1	FL	M280	M440
Gal4 DBD		1.0	0.9	1.1	1.0	1.1	1.1	0.9
Gal4 HNF-4(E)		18.2	9.8	5.1	23.5	2.8	22.6	3.5
Gal4 HNF-4(E354)		1.2	1.1	1.3	1.1	1.0	0.9	1.2
Gal4 VP16		159.0	143.5	150.8	182.7	178.5	185.2	175.6

Fig. 5. HNF-1 interacts with the AF2 domain of HNF-4 in vitro and in vivo. (A) In vitro synthesized [³⁵S]methionine-labeled HNF-1 was incubated with the indicated GST fusion proteins, and the bound proteins were analyzed by 10% SDS-polyacrylamide gel electrophoresis (PAGE). Growth and expression of GST fusion proteins in *Escherichia coli* strain JM109 were performed as described (15). ³⁵S-labeled full-length recombinant HNF-1 was synthesized in vitro from the corresponding constructs in Bluescript KS (Stratagene) using the TNT coupled reticulocyte lysate system (Promega). Glutathione-Sepharose beads containing 2 μg of each fusion protein were incubated with ³⁵S-labeled proteins in interaction buffer [100 mM KCl, 20 mM Hepes (pH 7.9), 0.1% NP-40, 5 mM MgCl₂, 0.2% bovine serum albumin (BSA), 10% glycerol, 0.1 M phenylmethylsulfonyl fluoride, and aprotinin (10 μg/ml)] for 1.5 hours at 4°C with constant agitation. After extensive washing with the same buffer minus BSA and glycerol, the beads were resuspended in 20 μl of SDS-loading buffer and analyzed by SDS-PAGE; 8% of the input ³⁵S-labeled HNF-1 is shown in the first lane. (B) COS-1 cells were transfected with 500 ng of nuclear localization-deficient mutant pMT-HNF-4(227-455) alone (pCB6 vector) or with 1 μg of pCB-HNF-1 FL, pCB-HNF-1(440), pCB-HNF-1(280), or pBx-Gal4 expression vectors, transferred to cover slips, and stained with polyclonal peptide antibody raised against the COOH-terminal 11-amino acid epitope of HNF-4, as described (14). The number of cells examined showing [nuclear]:[nuclear plus cytoplasmic]:[cytoplasmic] staining was 0:0:54 in HNF-4(227-455)-transfected cells. In cotransfected cells this ratio was 56:2:1 (HNF-1 FL), 51:1:2 [HNF-1(440)], 0:0:42 [HNF-1(280)], and 0:0:51 (Gal4). Typical examples of the immunofluorescent images are shown (magnifications, ×284).



ity to the transcription machinery or its direct interaction with general transcription factors. As a consequence, increased amounts of HNF-1 induce a regulatory mechanism that leads to the general down-regulation of HNF-4-dependent liver-specific genes, including the HNF-1 gene itself. This promoter-dependent dual function of HNF-1 suggests its central role in the coordination of the regulatory network that defines the hepatic phenotype.

REFERENCES AND NOTES

1. M. Frain *et al.*, *Cell* **59**, 145 (1989); S. Baumhueter *et al.*, *Genes Dev.* **4**, 372 (1990); V. De Simone *et al.*, *EMBO J.* **10**, 1435 (1991); W. H. Landschulz, P. F. Johnson, E. Y. Adashi, B. J. Graves, S. L. McKnight, *Genes Dev.* **2**, 786 (1988); E. Lai *et al.*, *ibid.* **4**, 1427 (1990); F. M. Sladek, W. Zhong, E. Lai, J. E. Darnell Jr., *ibid.*, p. 2353.
2. C. J. Kuo *et al.*, *Nature* **355**, 457 (1992); H.-M. Tian and U. Schibler, *Genes Dev.* **5**, 2225 (1991).
3. A. A. Kritis, E. Ktistaki, D. Barda, V. I. Zannis, I. Talianidis, *Nucleic Acids Res.* **21**, 5882 (1993).
4. G. Piaggio *et al.*, *ibid.* **22**, 4284 (1994).
5. M. Mietus-Snyder *et al.*, *Mol. Cell. Biol.* **12**, 1708 (1992); J. A. A. Ladias *et al.*, *J. Biol. Chem.* **267**, 15849 (1992); I. Talianidis, A. Tambakaki, J. Tourounova, V. I. Zannis, *Biochemistry* **34**, 10298 (1995).
6. F. Tronche *et al.*, in *Liver Gene Expression*, F. Tronche and M. Yaniv, Eds. (Landes, Austin, TX, 1994), chap. 9.
7. W. Zhong, J. Mirkovitch, J. E. Darnell Jr., *Mol. Cell. Biol.* **14**, 7276 (1994).
8. M. Pontoglio *et al.*, *Cell* **84**, 575 (1996).
9. D. B. Mendel *et al.*, *Science* **254**, 1762 (1991).
10. E. Ktistaki and I. Talianidis, unpublished data.
11. M. F. Carey, H. Kakidani, J. Leatherwood, F. Mostashari, M. Ptashne, *J. Mol. Biol.* **209**, 423 (1989).
12. F. M. Sladek, in (6), chap. 11.
13. E. Ktistaki, J. M. Lacorte, N. Katrakili, V. I. Zannis, I. Talianidis, *Nucleic Acids Res.* **22**, 4689 (1994); E. Ktistaki, N. T. Ktistakis, E. Papadogeorgaki, I. Talianidis, *Proc. Natl. Acad. Sci. U.S.A.* **92**, 9876 (1995); A. A. Kritis *et al.*, *Gene* **173**, 275 (1996).
14. E. Ktistaki and I. Talianidis, *Mol. Cell. Biol.* **17**, 2790 (1997).
15. D. B. Smith and K. S. Johnson, *Gene* **67**, 31 (1988).
16. We thank A. Economou for critical reading of the manuscript. Supported by Greek General Secretary for Science and Technology grant PENED2018.

7 February 1997; accepted 13 May 1997

Positive Effects of Combined Antiretroviral Therapy on CD4⁺ T Cell Homeostasis and Function in Advanced HIV Disease

B. Autran,* G. Carcelain, T. S. Li,† C. Blanc,† D. Mathez, R. Tubiana, C. Katlama, P. Debré, J. Leibowitch

Highly active antiretroviral therapy (HAART) increases CD4⁺ cell numbers, but its ability to correct the human immunodeficiency virus (HIV)-induced immune deficiency remains unknown. A three-phase T cell reconstitution was demonstrated after HAART, with: (i) an early rise of memory CD4⁺ cells, (ii) a reduction in T cell activation correlated to the decreasing retroviral activity together with an improved CD4⁺ T cell reactivity to recall antigens, and (iii) a late rise of "naïve" CD4⁺ lymphocytes while CD8⁺ T cells declined, however, without complete normalization of these parameters. Thus, decreasing the HIV load can reverse HIV-driven activation and CD4⁺ T cell defects in advanced HIV-infected patients.

New antiretroviral therapies combining inhibitors of HIV-1 protease and reverse transcriptase are highly efficient at reducing viral replication and increasing CD4⁺ T cell numbers (1). The physiopathological processes that allow such CD4⁺ T cell increases are debated as is the capacity of such treatments to allow CD4⁺ cell regeneration

and restoration of immune competence. These sets of questions reflect current controversies about the pathogenesis of HIV-related CD4⁺ cell depletion. Indeed, although much attention has been paid to the high turnover in HIV virions and infectious CD4⁺ T cells (2), no evidence for an enhanced turnover and regeneration in the mature CD4⁺ subset has been produced so far, either in the course of the natural HIV infection or after HAART (3). Telomere length studies have indeed provided evidence for a high turnover in the CD8⁺ but not in the CD4⁺ subset (4). Furthermore, reduced numbers of phenotypically defined "naïve" T cells in advanced HIV-infected patients argue for a decline in the T cell regeneration capacity with disease progression, although mechanisms for such defects

are not elucidated (5). On the other hand, the chronic T cell activation observed throughout the course of infection favors T cell apoptosis or anergy, or both, which might contribute to the CD4⁺ T cell depletion, though also affecting the undepleted CD8⁺ cell subset (6). A progressive CD4⁺ cell dysfunction also appears on a per-cell basis in early stages of the disease, as assessed in vitro by defects in CD4⁺ T cell proliferation and interleukin-2 (IL-2) production to recall antigens (7), and might participate in the loss of mature T cell expansion with disease progression.

We investigated the extent to which HAART would reverse these major CD4⁺ T cell abnormalities and allow some restoration of immune competence at advanced stages of HIV disease. We analyzed expression of key surface molecules on peripheral blood T cells and the CD4⁺ T cell proliferation against recall antigens from two major opportunistic infections under potent antiretroviral regimens. Eight previously untreated adults with advanced HIV-1 infection received zidovudine, a potent HIV-1 protease inhibitor, combined with zalcitabine (AZT) and didanosine, two reverse transcriptase inhibitors, over a period of 12 months. Zidovudine given alone the first 2 weeks rapidly induced a 1.3 ± 0.5 log decrease ($P = 0.01$) in the numbers of both HIV RNA copies per milliliter of plasma and infectious cells per 10^7 blood mononuclear cells from base-line values of 4.9 ± 0.4 and 3.4 ± 0.5 , respectively ($P < 0.05$). A maximal decline of 1.9 ± 0.6 log and 2.5 ± 0.5 log was reached for each viral parameter at month 6 under triple-combination therapy (Fig. 1). A low stable viral load was maintained under treatment through month 12 with plasma HIV-1 RNA copies falling below the threshold of detection in three of the eight patients. Major T cell changes were also observed in the peripheral blood from all patients during the first 2 weeks of treatment. A steep rise occurred in lymphocyte counts that predominated on the CD4⁺ subset, with a twofold CD4⁺ cell increase from a mean base line of 164 ± 86 cells/ μ l of plasma to 327 ± 74 cells/ μ l of plasma ($P = 0.01$). Meanwhile, CD8⁺ cells also increased, though with a lower amplitude from a mean of 1168 ± 427 cells/ μ l plasma at entry to 1387 ± 619 cells/ μ l plasma at day 15 ($P = 0.035$). During the next 12 months, a sustained though slower CD4⁺ cell increase was observed with a mean positive linear slope of +10%. The CD4⁺ cells reached a mean value of 365 ± 145 cells/ μ l plasma 1 year after initiation of the study, however, remaining below normal ranges in six of the eight patients (mean normal CD4 counts were 900 ± 185 cells/ μ l plasma). In contrast, CD8⁺ cells, as

B. Autran, G. Carcelain, T. S. Li, C. Blanc, P. Debré, Laboratoire d'Immunologie Cellulaire, URA CNRS 625, Hôpital Pitié-Salpêtrière, 47-83 Boulevard de l'Hôpital, Paris, France.

D. Mathez and J. Leibowitch, Service d'Immunologie Hématologie, Hôpital Raymond Poincaré, Garches, France. R. Tubiana and C. Katlama, Service de Maladies Infectieuses et Tropicales, Hôpital Pitié-Salpêtrière, Paris, France.

*To whom correspondence should be addressed. E-mail: autran@psi.ap-hop-paris.fr

†These authors contributed equally to this work.